symmetry

MDPI

Article

Utilization of Second Order Slip, Activation Energy and Viscous Dissipation Consequences in Thermally Developed Flow of Third Grade Nanofluid with Gyrotactic Microorganisms

Zahra Abdelmalek [1,2], Sami Ullah Khan [3], Hassan Waqas [4], Hossam A. Nabwey [5,6] and Iskander Tlili [7,8,*]

1 Institute of Research and Development, Duy Tan University, Da Nang 550000, Vietnam; zahraabdelmalek@duytan.edu.vn
2 Faculty of Medicine, Duy Tan University, Da Nang 550000, Vietnam
3 Department of Mathematics, COMSATS University Islamabad, Sahiwal 57000, Pakistan; sk_iiu@yahoo.com
4 Department of Mathematics, Government College University Faisalabad 38000, Pakistan; syedhasanwaqas@hotmail.com
5 Department of Mathematics, College of Science and Humanities in Al-Kharj, Prince Sattam bin Abdulaziz University, Al-Kharj 11942, Saudi Arabia; eng_hossam21@yahoo.com
6 Department of Basic Engineering Science, Faculty of Engineering, Menoufia University, Shebin El-Kom 32511, Egypt
7 Department for Management of Science and Technology Development, Ton Duc Thang University, Ho Chi Minh City 758307, Vietnam
8 Faculty of Applied Sciences, Ton Duc Thang University, Ho Chi Minh City 758307, Vietnam
* Correspondence: iskander.tlili@tdtu.edu.vn

Received: 13 January 2020; Accepted: 13 February 2020; Published: 21 February 2020

Abstract: In recent decades, an interest has been developed towards the thermal consequences of nanofluid because of utilization of nano-materials to improve the thermal conductivity of traditional liquid and subsequently enhance the heat transportation phenomenon. Following this primarily concept, this current work investigates the thermal developed flow of third-grade nanofluid configured by a stretched surface with additional features of activation energy, viscous dissipation and second-order slip. Buongiorno's nanofluid model is used to explore the thermophoresis and Brownian motion features based on symmetry fundamentals. It is further assumed that the nanoparticles contain gyrotactic microorganisms, which are associated with the most fascination bioconvection phenomenon. The flow problem owing to the partial differential equations is renovated into dimensional form, which is numerically simulated with the help of bvp4c, by using MATLAB software. The aspects of various physical parameters associated to the current analysis are graphically examined against nanoparticles' velocity, temperature, concentration and gyrotactic microorganisms' density distributions. Further, the objective of local Nusselt number, local Sherwood number and motile density number are achieved numerically with variation of various parameters. The results presented here may find valuable engineering applications, like cooling liquid metals, solar systems, power production, solar energy, thermal extrusion systems cooling of machine equipment, transformer oil and microelectronics. Further, flow of nanoparticles containing gyrotactic microorganisms has interesting applications in microbial fuel cells, microfluidic devices, bio-technology and enzyme biosensors.

Keywords: bioconvection; slip flow; third-grade nanofluid; microorganism; activation energy

1. Introduction

In the 21st century, a considerable amount of attention has been paid to nanotechnology, which is the most emerging scientific area of research and has is of industrial and engineering significance. The nanofluids with effective thermal characteristics are engaged in fundamental applications like solar systems, power collectors, material processing, as a coolant, medical agents, nuclear reactors, chemical industries, geo-thermal engineering, petroleum industries, etc. The feature that makes the nanofluid more versatile is the use of such metallic nanoparticles to enhance the thermal extrusion system and manufacturing processes in various industrial products. Beside this, nanofluids signify the significance in the material fabrication because they are considered to be biologically friendly, durable and sustainable products. Recently, a variety of experimental and theoretical computations were performed to explore the thermophysical aspects of such nanoparticles. The term "nanofluid", a suspension of nanoparticles with liquids, was coined by Choi [1]. Later on, Buongiorno [2] claimed that convective heat transfer of nanofluid is characterized by seven slip mechanisms, which mainly include Brownian motion and thermophoresis diffusion. The mechanism of heat transportation based on flow of nanoparticles cannot be completely investigated without these important diffusion coefficients. Sandeep and Sulochana [3] predicted the simultaneous thermophysical features in three types of viscoelastic fluids, namely Maxwell fluid, Oldroyd-B fluid and Jeffrey fluid, additionally featuring the heat absorption and generation consequences. The thermally developed flow of micropolar nanofluid with impact of heat source and sink has been numerically attempted by Pal and Mandal [4]. Khan et al. [5] implemented mass flux constraints in diffusion of rate type nanoparticles with influence of thermal radiation. The suspension of water-based nanoparticles induced by rotating disk with variable thickness and melting heat transfer was reported by Hayat and co-workers [6]. Tlili et al. [7] examined the heat transfer characteristics in the flow of aluminum oxide and copper nanoparticles with suspension of sodium alginate base liquid. The modeled problem was numerically simulated by using shooting technique. The study focused by Khan and Shehzad [8] deals with the thermophoresis and Brownian motion aspects in flow of third-grade nanofluid induced by periodically moving accelerated surface. Waqas et al. [8] investigated the rheological significance of Maxwell and micropolar nanoparticles in the presence of porous space where a modeled problem was numerically preceded. Another theoretical continuation examining the viscous dissipation and magnetic force features was numerically examined by Hsiao [9]. Sheikholeslami and Bhatti [10] interpolated the shape feature effect in force convection flow of nanoparticles influenced by magnetic force. Turkyilmazoglu [11] studied the thermophysical properties in the flow of both single- and double-phase nanofluid models encountered by concentric annuli.

The phenomenon of "bioconvection" is associated with the macroscopic motion of particles which results from the collective swimming of microorganism due to density gradient. The movement of such microorganism is self-impelled due to which the density of base liquid improves in some specific direction. This variation in the base fluid density due to involvement of microorganism is termed as bioconvection, and recently, a considerable deviation on this topic has been intended by researchers. The microorganisms are classified into oxytactic, negative gravitaxis, chemo-taxis and gyrotactic microorganisms based on impellent factor. Unlike such microorganisms' movement, the deviation in nanoparticles is not self-originated, but their movement is associated with the most important factors of thermophoresis factor and Brownian diffusion. The applications of bioconvection phenomenon include bio-fuels, drug delivery, enzymes, bio-technology, biosensors and nano-biotechnology. The primary contribution which deals with the bioconvection of nanoparticles was directed by Kuznetsov [12,13] in which it is claimed that the presence of gyrotactic microorganisms in nanoparticles can be improve the density stratification. Uddin et al. [14] incorporated the suction and injection features in slip flow of nanofluid with gyrotactic microorganisms induced by a moving surface. Xun et al. [15] anticipated the bio-convective of nanoparticles configured by a rotating system where the impact of viscosity is assumed to be temperature dependent. Another mathematical model which reports the bioconvection aspects in Casson nanoparticles under the influence of thermal radiation was formulated by Raju

et al. [16]. Alsaedi et al. [17] reported the bioconvection flow of magneto-nanoparticles induced by a convectively heated stretched configuration. The flow caused due to truncated cone carrying nanoparticles and gyrotactic microorganisms was checked out by Khan et al. [18]. The bioconvection aspects associated with the generalized second-grade nanofluid flow has been reported by Waqas et al. [19]. Another work based on the bioconvection of nanoparticles featuring activation energy and slip impact in flow of Eyring Powell non-Newtonian fluid has been analyzed by Alwatban et al. [20]. Tlili et al. [21] proposed a theoretical model for the stretched flow of Oldroyd B nanofluid in presence of gyrotactic microorganism. They also employed second-order slip features, namely Wu's slip, which leads to a truncation of associated boundary layers. The mixed convection flow of nanoparticles in horizontal channel containing gyrotactic microorganisms has been studied by Xu and Pop [22]. Sheremet and Pop [23] investigated thermo-bioconvection in nanoparticles configured by a porous cavity.

The dynamic of non-Newtonian fluids is quite interesting due to interdisciplinary rheological features and complex physical properties; it has attained special attention of researchers in recent days. From the flow of non-Newtonian fluids emerged a variety of interesting applications, like polymer solutions, slurries, biological fluids, blood, lubrication, chemical industries, etc. It is commonly visualized that these fluids show a nonlinear behavior which cannot be predicted via simple mean. Among these models, third-grade fluid is one which attributes the shear thickening/shear thinning features effectively. The Cauchy stress tensor for third-grade fluid can be defined as follows [24]:

$$\mathbf{T} = -p\mathbf{I} + \mu\mathbf{A}_1 + \alpha_1\mathbf{A}_2 + \alpha_2\mathbf{A}_1^2 + \beta_3(tr\mathbf{A}_1^2)\mathbf{A}_1, \tag{1}$$

where represents the pressure; $\mathbf{I}$ is for identity tensor; μ is the dynamic viscosity; $(\mathbf{A_1}, \mathbf{A_2})$ denotes the Rivlin–Ericksen tensors; and α_1, α_2 and β_3 are material constants which have following relations:

$$\mu \geq 0, \quad \alpha_1^* \geq 0, \quad \beta_1 = \beta_2 = 0, \quad \beta_3 \geq 0, \quad \alpha_1^* + \alpha_2^* \leq \sqrt{24\mu\beta_3}, \tag{2}$$

The Rivlin–Ericksen tensors $\mathbf{A_1}$ and $\mathbf{A_2}$ are defined as follows:

$$\mathbf{A}_1 = \mathbf{L} + \mathbf{L}^\mathbf{t}, \mathbf{L} = \nabla\mathbf{V}, \tag{3}$$

$$\mathbf{A}_2 = \frac{d\mathbf{A}_1}{dt} + \mathbf{A}_1\mathbf{L} + \mathbf{L}^\mathbf{t}\mathbf{A}_1, \tag{4}$$

A variety of work based on the rheological features of third-grade fluid is attributed in references [25–27].

Following such valuable applications of bioconvection of magnetized nanoparticles, we analyzed the flow of third-grade nanofluid with gyrotactic microorganisms over a stretched surface in presence of second-order slip constraints. Additionally, the viscous dissipation, activation energy and thermal radiation effects are also reported on the current simulations. The governing dimensionless flow problem is numerically simulated by adopting the shooting procedure. The effects of physical parameters governing the current flow situations are graphically impacted with justified relevant significance and are based on the symmetry concept.

2. Mathematical Modelling

Let us study bioconvection prospective in third-grade nanofluid flow induced by a stretched surface in the *xy*-plane. The considered fluid is assumed to be electrically conducting where magnetic field effects are imposed by a normally directed uniform magnetic field. For thermally developed flow, the consequences of thermal radiation are inspected by using Rosseland approximations. The activation energy prospective is also utilized with evaluation of Arrhenius chemical reaction relations. The flow is subjected to the Wu's slip, for which relevant expressions are used coinciding two slip parameters. Moreover, the convective Nield's boundary constraints has been suggested for the temperature and

concentration distributions of nanoparticles. The free-stream nanoparticles' temperature, concentration and motile microorganism are respectively represented by T_∞, C_∞ and N_∞. Based on such assumptions, the governing flow equations for the evaluated flow problem can be expressed in following forms:

$$\frac{\partial u}{\partial x}+\frac{\partial v}{\partial y}=0, \tag{5}$$

$$\begin{aligned} u\frac{\partial u}{\partial x}+v\frac{\partial u}{\partial y}&=\nu\frac{\partial^2 u}{\partial y^2}+\frac{\alpha_1}{\rho_f}\left(v\frac{\partial^3 u}{\partial y^3}+\frac{\partial u}{\partial x}\frac{\partial^2 u}{\partial y^2}+u\frac{\partial^3 u}{\partial x\partial y^2}+\frac{\partial u}{\partial y}\frac{\partial^2 v}{\partial y^2}\right)-\frac{\sigma {B_0}^2}{\rho_f}u\\ &+\frac{6\beta_3}{\rho_f}\left(\frac{\partial u}{\partial y}\right)^2\frac{\partial^2 u}{\partial y^2}+\frac{1}{\rho_f}\left[\begin{array}{c}\left(1-C_f\right)\rho_f\beta^*g^*(T-T_\infty)-\left(\rho_p-\rho_f\right)g^*(C-C_\infty)\\ -(N-N_\infty)g\gamma^{**}\left(\rho_m-\rho_f\right)\end{array}\right], \end{aligned} \tag{6}$$

$$\begin{aligned} u\frac{\partial T}{\partial x}+v\frac{\partial T}{\partial y}&=\left(\alpha_e+\frac{16\sigma^*T_\infty^3}{3k^*(\rho c)_f}\right)\frac{\partial^2 T}{\partial y^2}+\frac{\left(\rho c_p\right)_p}{\left(\rho c_p\right)_f}\left\{D_B\frac{\partial T}{\partial y}\frac{\partial C}{\partial y}+\frac{D_T}{T_\infty}\left(\frac{\partial T}{\partial y}\right)^2\right\}+\frac{\sigma {B^2}_0}{(\rho c)_f}u^2+\\ &\frac{\mu}{\left(\rho c_p\right)_f}\left(\frac{\partial u}{\partial y}\right)^2+\frac{\alpha_1}{\left(\rho c_p\right)_f}\left(u\frac{\partial u}{\partial y}\frac{\partial^2 u}{\partial x\partial y}+v\frac{\partial u}{\partial y}\frac{\partial^2 u}{\partial^2 y}\right)+\frac{2\beta_3}{\left(\rho c_p\right)_f}\left(\frac{\partial u}{\partial y}\right)^4, \end{aligned} \tag{7}$$

$$u\frac{\partial C}{\partial x}+v\frac{\partial C}{\partial y}=D_B\frac{\partial^2 C}{\partial y^2}+\frac{D_T}{T_\infty}\frac{\partial^2 T}{\partial y^2}-K_1r^2(C-C_\infty)\left(\frac{T}{T_\infty}\right)^2\exp\left(\frac{-E_a}{\kappa T}\right), \tag{8}$$

$$u\frac{\partial N}{\partial x}+v\frac{\partial N}{\partial y}+\frac{bW_c}{(C_w-C_\infty)}\left[\frac{\partial}{\partial y}\left(N\frac{\partial C}{\partial y}\right)\right]=D_m\left(\frac{\partial^2 N}{\partial y^2}\right), \tag{9}$$

The important physical quantities appeared above can be defined as, u reports velocity component in $x-$direction, v represents the component of velocity along $y-$direction, ν is kinematic viscosity, ρ_f is the fluid density, β^* volume expansion coefficient, g^* gravity, ρ_p is the nanoparticles density, ρ_m is the microorganisms particles density, T is the temperature, C represents the concentration, N microorganisms density, α_e thermal diffusivity, k^* mean absorption coefficients, $\sigma*$ Stephan-Boltzmann, $(\rho c)_f$ is effective heat capacity of base fluid, $(\rho c)_p$ effective heat capacity of nanoparticles, D_B reports the diffusion constant, B_0 represents the magnetic field intensity, D_m is the diffusivity of micro-organisms, γ^{**} is average volume of a microorganism, D_T thermodiffusion constant, K_1r reaction rate, κ Boltzmann constant, E_a activation energy, W_e is speed of cells while b_1 denotes the chemotaxis constant.

The following boundary conditions are structured to the current flow problem:

$$u=u_w+u_{slip},\quad v=0,\quad -k\frac{\partial T}{\partial y}=h_f\left(T_f-T\right),\quad D_B\frac{\partial C}{\partial y}+\frac{D_T}{T_\infty}\frac{\partial T}{\partial y}=0,\ N=N_w,\ \text{at } y=0, \tag{10}$$

$$u\to U_\infty=0,\ v\to 0,\ T\to T_\infty,\ C\to C_\infty,\ N\to N_\infty\ at\ y\to\infty, \tag{11}$$

where h_f represents the heat transfer coefficient, while T_f is the convective fluid temperature. The slip effects in the current flow situation are considered in form of second order, which was originally developed by Wu [28], and later on, some interesting contributions were proceeded by numerous investigators [29–32].

$$u_{slip}=\frac{2}{3}\left(\frac{3-\Gamma l^2}{\Gamma}-\frac{3}{2}\frac{1-l^2}{k_n}\right)\varepsilon\frac{\partial u}{\partial y}-\frac{1}{4}\left[l^4+\frac{2}{k_n^2}\left(1-l^2\right)\right]\varepsilon^2\frac{\partial^2 u}{\partial y^2}, \tag{12}$$

$$u_{slip}=A\frac{\partial u}{\partial x}+G\frac{\partial^2 u}{\partial x^2} \tag{13}$$

where k_n notify the Knudsen number, $l=\min\left[\frac{1}{k_n},1\right]$, Γ is the momentum coefficient with and ε molecular mean free path. Following to the definition of l, it was observed that, for k_n assigned values, we should $0\le l\le 1$. It is remarked that molecular mean free path is always positive [32].

Following this, similarity quantities are incorporated in order to attained the dimensionless form of the governing equations:

$$\begin{aligned}&\zeta = \sqrt{\tfrac{a}{\nu}}y, u = cxf'(\zeta), v = -\sqrt{c\nu}f(\zeta),\ \theta(\zeta) = \tfrac{T-T_\infty}{T_w-T_\infty},\\&\phi(\zeta) = \tfrac{C-C_\infty}{C_\infty}, \chi(\zeta) = \tfrac{N-N_\infty}{N_w-N_\infty},\end{aligned} \tag{14}$$

While inserting the above variables in the governing flow Equations (6)–(9), one yields the following:

$$\begin{aligned}&f''' - (f')^2 + ff'' - Mf' + K\Big(2f'f''' - ff^{iv} - (f'')^2\Big) + \Lambda(\theta - Nr\phi - Nc\chi)\\&+6\Omega \mathrm{Re} f'''f''^2 = 0,\end{aligned} \tag{15}$$

$$\begin{aligned}&\Big(\tfrac{1}{\mathrm{Pr}} + \tfrac{4}{3}Rd\Big)\theta'' + Nb\theta'\phi' + f\theta' + Nt\theta'^2 + Ecf''^2 + MEcf'^2\\&+KEc\Big(f'f''^2 - ff''f'''\Big) + 2Ec\Omega\mathrm{Re}f''^4 = 0,\end{aligned} \tag{16}$$

$$\phi'' + \Big(\frac{Nt}{Nb}\Big)\theta'' + Le\mathrm{Pr}f'\phi + \Big(\frac{Nt}{Nb}\Big)\theta'' - Le\mathrm{Pr}\sigma^{**}(1+\delta\theta)^n\phi\exp\Big(-\frac{E}{1+\delta\theta}\Big) = 0, \tag{17}$$

$$\chi'' + Lbf\chi' - Pe(\phi''(\chi+\delta_1) + \chi'\phi') = 0. \tag{18}$$

The abovementioned transmuted equations acquire a flowing set of boundary conditions:

$$\left.\begin{aligned}&f(0) = 0, \quad f'(0) = 1 + \alpha f''(0) + \beta f'''(0), \quad \theta'(0) = Bi(\theta(0) - 1),\\&Nb\theta'(0) + Nt\phi'(0) = 0, \quad \chi(0) = 1,\\&f'(\infty) \to 0, \quad \theta(\infty) \to 0, \quad \phi(\infty) \to 0, \quad \chi(\infty) \to 0.\end{aligned}\right\} \tag{19}$$

where M is Hartmann number, K is material parameter, Λ mixed convection parameter, Nr buoyancy ratio parameter, Nc bioconvection Rayleigh number, Re is Reynolds number, Ω is third grade fluid parameter, Pr Prandtl number, Rd radiation parameter, Nb Brownian motion parameter, Nt thermophoresis parameter, Ec Eckert number, Le Lewis number, σ^{**} is reaction constant, δ temperature difference parameter, E activation energy parameter, δ_1 specify microorganism concentration difference constant, Pe is Peclet number, Lb determine the bioconvection Lewis number, Bi is thermal Biot number while α and β first order slip and second order slip constants which are mathematically related into following forms:

$$M = \sqrt{\tfrac{\sigma B_0^2}{c\rho_f}}, \mathrm{K} = \tfrac{c\alpha_1}{\mu}, Nr = \tfrac{(\rho_p-\rho_f)(C_w-C_\infty)}{\beta\rho_f(1-C_\infty)T_\infty}, Nc = \tfrac{\gamma(\rho_m-\rho_f)(N_w-N_\infty)}{\beta\rho_f(1-C_\infty)T_\infty}, \Omega = \tfrac{c^2\beta_3}{\mu},$$

$$\mathrm{Re} = \tfrac{cx^2}{\nu}, \mathrm{Pr} = \tfrac{\nu}{\alpha_e}, Rd = \tfrac{4\sigma^*T_\infty^3}{kk^*}, Nt = \frac{\big(\rho c_p\big)_p D_B\big(T_f-T_\infty\big)}{T_\infty\nu\big(\rho c_p\big)_f}, \Lambda = \left(\frac{(T_\infty)\beta_1 g_1(1-C_\infty)}{c(\rho c)_f}\right)$$

$$Nb = \frac{\big(\rho c_p\big)_p D_B C_\infty}{\big(\rho c_p\big)_f \nu}, Ec = \frac{u_\infty^2}{c_p\big(T_f-T_\infty\big)}, Le = \tfrac{\alpha}{D_B}, Lb = \tfrac{\nu}{D_m}, Pe = \tfrac{bw_c}{D_m}, \mathrm{Bi} = \tfrac{h_f}{k}\sqrt{\tfrac{\nu}{c}},$$

$$\sigma = \tfrac{k_a}{c}, \delta = \tfrac{T_w-T_\infty}{T_\infty}, Pe = \tfrac{\widetilde{b}W_c}{D_m}, E = \tfrac{E_a}{K_1rT_\infty}, \gamma = \big(h_f/k\big)\sqrt{\nu/c}, \alpha = A\sqrt{\tfrac{c}{\nu}}, \delta = \tfrac{Gc}{\nu}.$$

The numerical values for local Nusselt number, local Sherwood number and motile density number can be calculated by using the following relations:

$$\mathrm{Re}^{-1/2}Nu_x = -\Big(1 + \frac{4}{3}R\Big)\theta'(0), \tag{20}$$

$$\mathrm{Re}^{-1/2}Sh_x = -\phi'(0), \tag{21}$$

$$\mathrm{Re}^{-1/2}N_n = -\chi'(0). \tag{22}$$

3. Numerical Scheme

This section signifies the numerical simulations of the dimensionless flow Equations (15)–(18), with boundary conditions defined in Equation (19). Since formulated equations are highly nonlinear, exact solution is not possible. For this purpose, we use a famous numerical approach, namely bvp4c, by using MATLAB software. In fact, this numerical method is a finite difference code which is associated with 3-stage Lobatto IIIa formulae. For this purpose, we convert higher-order boundary value problem into first-order initial values problem by following procedure:

$$
\begin{aligned}
&f = s_1, f' = s_2, f'' = s_3, f''' = s_4, f'''' = s_4', \quad \theta = s_5, \theta' = s_6, \theta'' = s_6', \phi = s_7,\\
&\phi' = s_8, \phi'' = s_8', \quad \chi = s_9, \chi' = s_{10}, \chi'' = s_{10}'\\
&s_4' = \frac{s_4 - (s_2)^2 + s_1 s_3'' - M s_2 - 2K s_2 s_4 - K s_3^2 + \Lambda \begin{pmatrix} s_5 - Nr s_7 \\ -Nc s_9 \end{pmatrix} + 6\Omega \mathrm{Ra} s_4 s_3^2}{K s_1}\\
&s_6' = \frac{-\left(f s_6 + Nb s_6 s_8 + Nt s_6^2 + Ec s_3^2 + MEc s_2^2 + KEc\left(s_2 s_3^2 - s_1 s_3 s_4\right) + 2Ec\Omega \mathrm{Ra} s_3^4\right)}{\left(\frac{1}{\mathrm{Pr}} + \frac{4}{3} Rd\right)}\\
&s_8' = -\left(\frac{Nt}{Nb}\right) s_6' - Le \mathrm{Pr} s_2 s_7 - \left(\frac{Nt}{Nb}\right) s_6'\\
&s_{10}' = -Lb s_1 s_{10} + Pe\left(s_8'(s_9 + \delta_1) + s_{10} s_8\right)\\
&s_1(0) = 0, s_2 = 1 + \alpha s_3(0) + \beta s_4(0), s_6 = \beta_i (s_5(0) - 1),\\
&Nb s_6(0) + Nt s_8(0) = 0, s_9(0) = 1 \quad as \quad \zeta = 0\\
&s_2 \to 0, s_5 \to 0, s_7 \to 0, s_9 \to 0, \quad as \quad \zeta \to 0
\end{aligned}
\tag{23}
$$

The numerical computations has been performed against various values of flow parameters with bounded domain $[0, \zeta_{\max}]$ instead of $[0, \infty)$ where value of $\zeta_{\max}$ is choosen in such way that there is no convincible change is noted in results for values larger than $\zeta_{\max}$. The iterative processes is controlled by using formula

$$
\max\left\{\left|h_2(\zeta_{\max}) - 0\right|, \left|h_4(\zeta_{\max}) - 0\right|, \left|h_6(\zeta_{\max}) - 0\right|, \left|h_8(\zeta_{\max}) - 0\right|\right\} < \xi, \tag{24}
$$

where ξ denotes a small real number. The iterative process has been utilized and the accuracy of solution is carefully examined up to 10^{-6}.

4. Results Validation

Present numerical simulations are validated with Turkyilmazoglu, in Table 1, as a limiting case. Here, an excellent agreement between both studies is noted.

Table 1. Comparison of solution for $f''(0)$ when $K = \mathrm{Re} = \Omega = Nr = Nc = Rb = 0$..

M	Turkyilmazoglu	Present Results
0	−1.000000	−1.000000
0.5	−1.224744	−1.224748
1	−1.414213	−1.414218
1.5	−1.581138	−1.581147
2.0	−1.732050	−1.732057

5. Discussion

This section deals with the physical significance of flow model constructed and simulated in previous sections. Now we examine the change in the nanoparticles velocity, nanoparticles temperature distribution, concentration distribution and microorganism density distribution for each flow parameter

like Hartmann number M, material parameter K, Grashoff number Λ, buoyancy ratio parameter Nr, bioconvection Rayleigh number Nc, Reynolds number Re, third grade fluid parameter Ω, Prandtl number Pr, radiation parameter Rd, Brownian motion parameter Nb, thermophoresis parameter Nt, Eckert number Ec, Lewis number Le, reaction constant σ^{**}, temperature difference parameter δ, activation energy parameter E, Peclet number Pe, bioconvection Lewis number Lb, microorganism concentration difference parameter δ_1, thermal Biot number Bi, first order slip factor α and second order slip β. For performing graphical analysis, one parameter varies while all the physical parameters are referred to some constant values like $M = 0.2$, $K = 0.2$, $\Lambda = 0.2$, $Nr = 0.4$, $Nc = 0.4$, Re $= 0.5$, $\Omega = 0.2$, Pr $= 0.5$, $Rd = 0.5$, $Nb = 0.5$, $Nt = 0.5$, $Ec = 0.5$, $Le = 0.5$,, $\sigma^{**} = 0.5$, $\delta = 0.5$, $E = 0.5$, $\delta_1 = 0.5$, $Pe = 0.5$, $Lb = 0.5$, $Bi = 0.5$, $\alpha = 0.5$ and $\beta = 0.5$.

The output which concern with the variation of Nr and Nc on f' is demonstrated in Figure 1. It is observed that increment in buoyancy ratio parameter Nr and bioconvection Rayleigh number Nc causes a reduction in the velocity profile. The physical explanation associated with such trend may attribute as both parameters involves the buoyancy ratio force which resists the association magnetized nano-particles in the flow region. The physical impact of slip factors α and β on f' has been studied in Figure 2. The change in the velocity distribution is altered due to interaction of slip effects. The increment of both slip factors show a decaying velocity distribution which is more progressive for α.

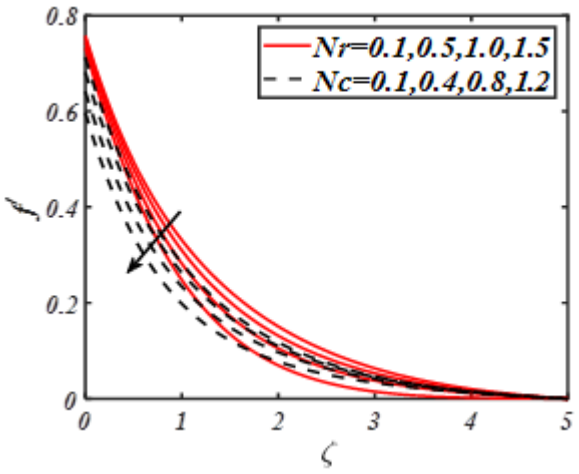

Figure 1. Change in f' with Nr and Nc..

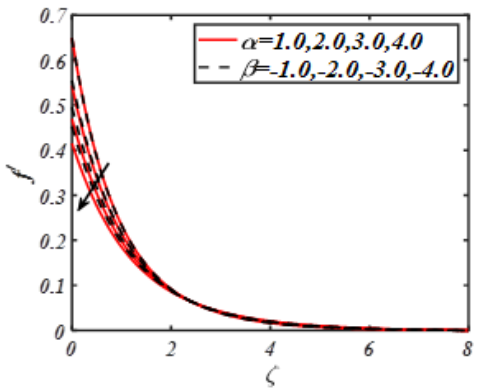

Figure 2. Change in f' with α and β.

Figure 3 exhibits the distinctions of temperature profiles θ for higher values of Prandtl number Pr and radiation parameter Rd. A depreciate temperature profile θ has been noted for progressive values of Pr. In fact Prandtl number captured is inversely relation with thermal diffusivity which reports a declining θ. However, in case of radiation parameter, an enhanced temperature distribution is noted.

Thermal radiation is the mode of heat transfer which utilizes some extra energy to the system which can be more helpful to improve the heat transfer phenomenon. The significance of thermal radiation includes many applications like solar energy systems and various extrusion processes. Figure 4 exhibits the impact of viscoelastic parameter K and third grade fluid parameter Ω on temperature distribution θ. The temperature distribution θ goes downturn with increase of both parameters due to presence of viscosity effects. However, the increment in θ is more dominant for K as compared to Ω. Figure 5 indicates the variation of Biot number Bi and thermophoresis parameter Nt on θ. Since Bi is directly related to the heat transfer coefficient which responded an improved temperature distribution. The change in θ is also more sufficient with variation of thermophoresis constant Nt. The thermophoresis phenomenon is encountered a diverse interesting compliance in many industrial processes. This phenomenon occurs due when heated fluid particles move to the lower temperature difference region and as result the temperature distribution get enlarge due to temperature difference. Figure 6 illustrates the effect of first order slip α and second order slip factor β on temperature distribution θ. The temperature profile get large with increment of both slip parameters. Now we analyze the impact of mixed convection Λ and Reynolds number Re on θ, Figure 7 is prepared. The variation in both parameters results a depressed temperature profile.

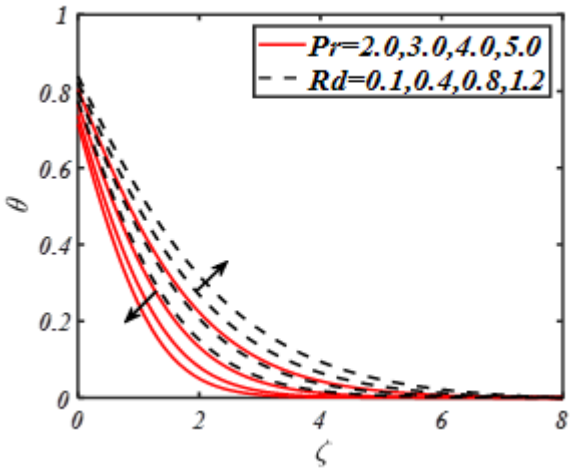

Figure 3. Change in θ with Pr and Rd.

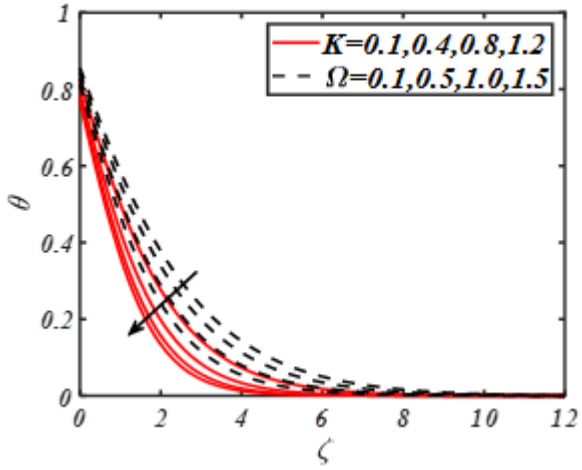

Figure 4. Change in θ with K and Ω.

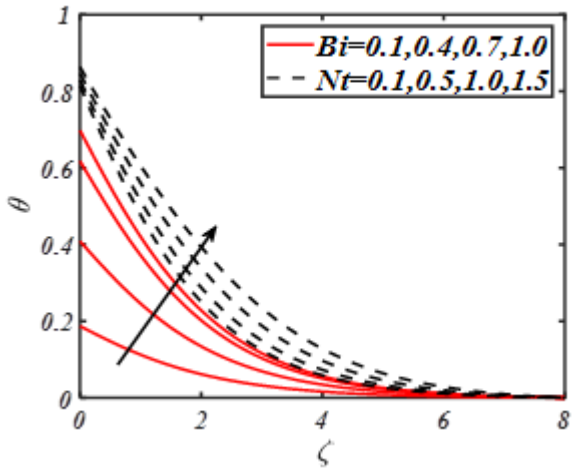

Figure 5. Change in θ with Bi and Nt.

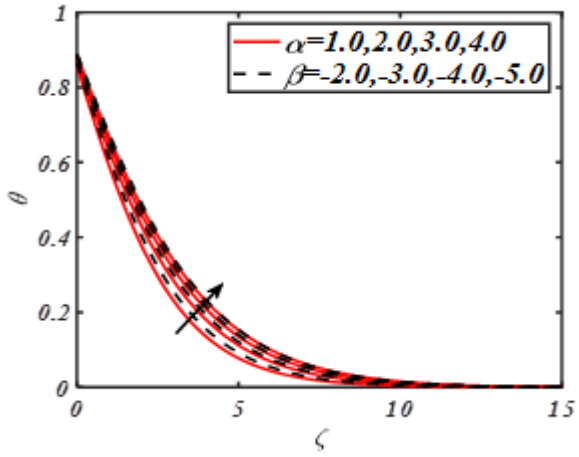

Figure 6. Change in θ with α and β.

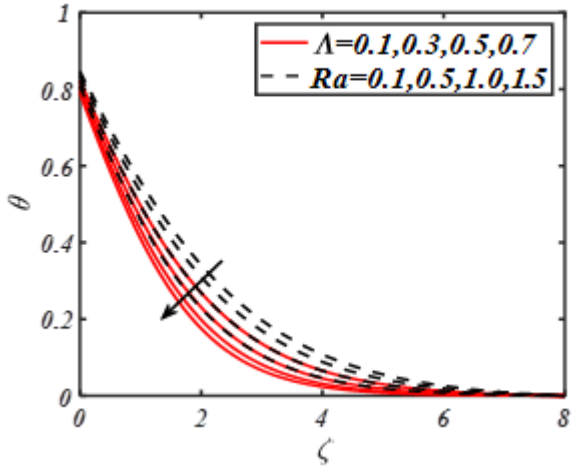

Figure 7. Change in θ with Λ and Re.

The importance of Brownian motion Nb and Lewis number Le concentration profile ϕ is displayed by Figure 8. A decreasing trend in concentration distribution ϕ is found out for larger values of Brownian motion Nb and Lewis number Le. The change in Nb involves the Brownian movement of fluid particles which decay the nanoparticles concentration ϕ. The impact of Le also leads to a decrement of ϕ as it Lewis number retained reverse relation with mass diffusivity. Therefore, slightly minimum mass

diffusivity is noted when *Le* get maximum variation. Figure 9 underlines the graphical prospective of Prandtl number *Pr* and activation energy *E* on concentration ϕ. Both parameters shows opposite trend on concentration distribution. With rising values of *Pr*, a lower variation in ϕ is resulted. The result portrayed for activation energy parameter *E* claimed an increasing concentration distribution. The activation energy signifies a prime implication in many reactive processes. The activation energy play a valuable roll to improve the reaction phenomenon. The importance of mixed convection parameter Λ and Reynolds number Re on ϕ is graphically deliberated in Figure 10. The prominent observation justified a declining profile of ϕ for both flow parameters. Figure 11 explore the variation in ϕ due to change in material parameter *K* and third grade fluid parameter Ω. By assigning numerical values to both material parameters, it is revealed that concentration profile ϕ decreases which is more dominant with variation of *K*. Physically, both parameters are associated with fluid viscosity which results a diminishing concentration profile. The roll of slip factors α and β on ϕ is presented in Figure 12 which shows that concentration distribution depressed with both slip factors α and β.

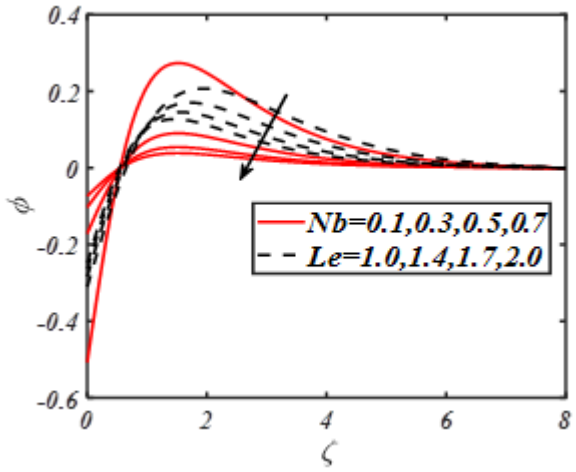

Figure 8. Change in ϕ for *Nb* and *Le*.

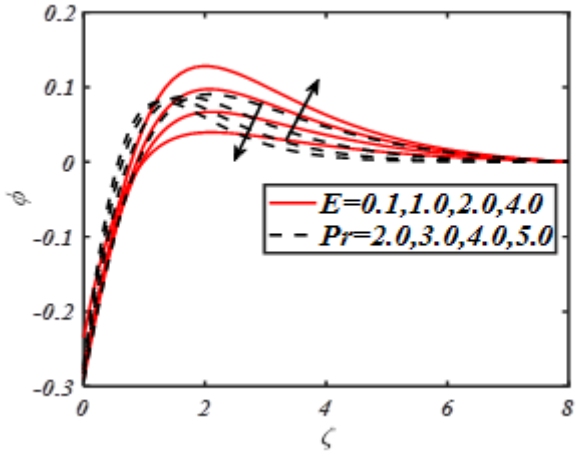

Figure 9. Change in ϕ for *E* and *Pr*..

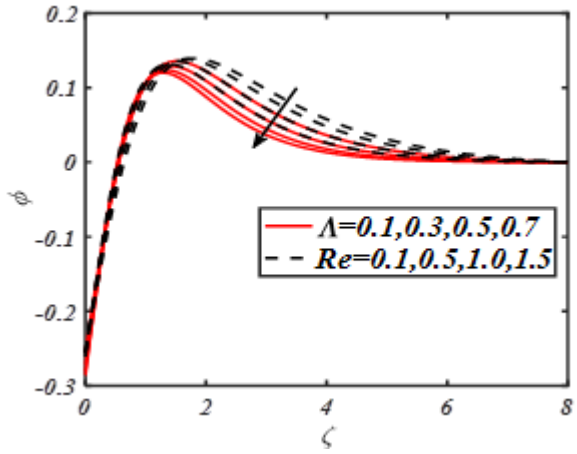

Figure 10. Change in ϕ for Λ and Re.

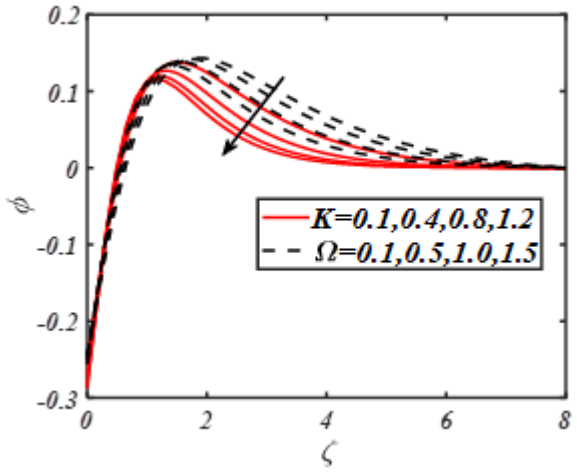

Figure 11. Change in ϕ for K and Ω.

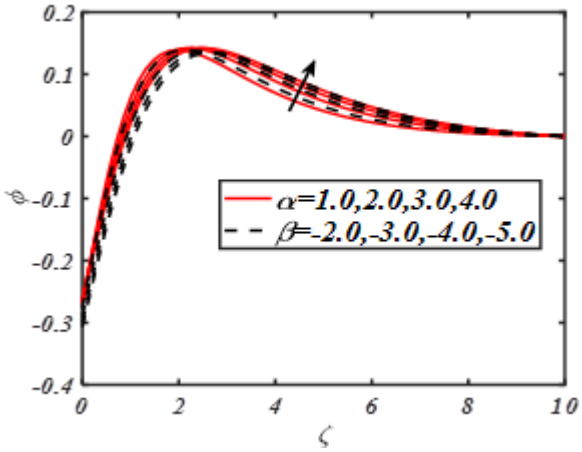

Figure 12. Change in ϕ for α and β.

The analysis for motile microorganism distribution χ for increasing numerical values of first order slip parameter α and second order slip factor β is depicted in Figure 13. A strengthened in χ is evaluated when both parameter enlarge increasing values. The effect of Reynolds number Re and mixed convection constant Λ on motile microorganism profile is drawn in Figure 14. Obtained results exhibiting a decreasing profile of χ due to variation of Reynolds number and mixed convection parameter. The effective convection result in small amount of motile distribution. To visualize the

impact of viscoelastic parameter K and third-grade fluid parameter Ω on motile microorganism distribution χ, we portrayed Figure 15. The demonstrated results report that when we uplift both parameters, the motility profile χ gives a declining trend. Figure 16 divulges the effect of bioconvection Lewis number Lb and Peclet number Pe on motile microorganism profile χ. As intensify the values of Lb and Pe results a declining motile microorganism distribution χ. The higher values of Pe corresponds to minimum motile diffusivity due to which a declining motile microorganisms profile χ is configured.

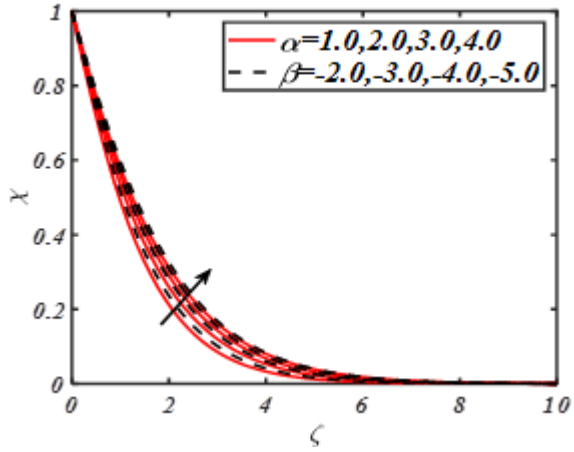

Figure 13. Change in χ for α and β.

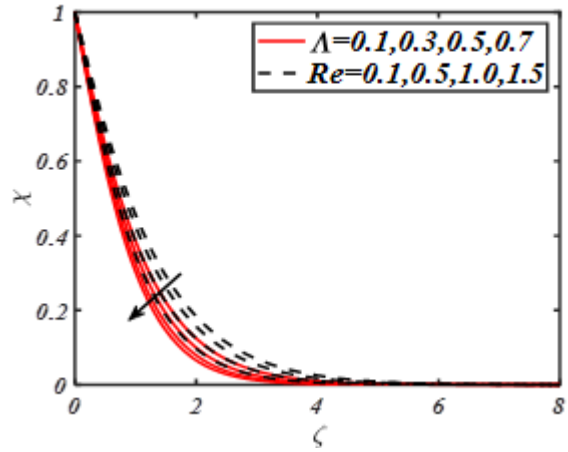

Figure 14. Change in χ for Λ and Re.

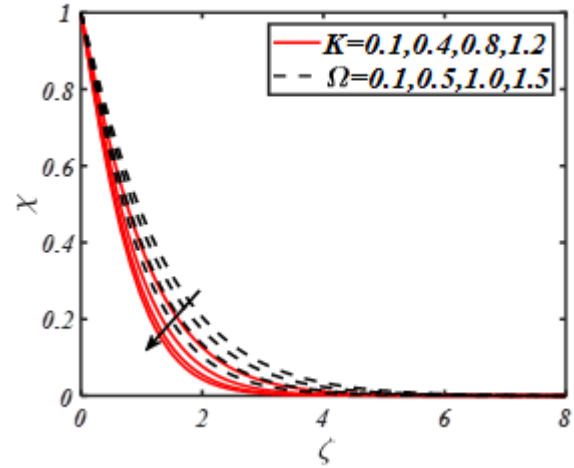

Figure 15. Change in χ for K and Ω.

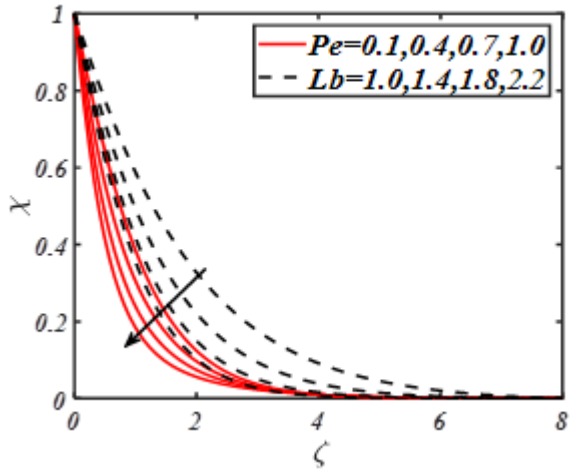

Figure 16. Change in χ for *Pe* and *Lb*.

The numerical results are reported in Table 2 for variation of $-f''(0)$ against various flow parameters like M, Ω, Nc, Nr, Re, α and β. It is examined that $-f''(0)$ get maximum values with increment of M while reverse trend is reported with variation of Re, α and β. Table 3 evaluates the impact of local Nusselt number $-\theta'(0)$ against variation of *Nb*, *Nt*, *Bi*, Pr, Λ, Re and Ω. With increase of *Nb*, *Nt* and Re, the change in local Nusselt number in lower in contrast to Pr and Λ. From Table 4 where change in local Sherwood number $-\phi'(0)$ is inspected which shows that $-\phi'(0)$ declined with *Nb*, *Nt* and Re while it increases with *Le* and Λ. Finally, from Table 5, it is reveal that the motile density number boost up with *Pe*, Λ and *Lb*.

Table 2. Numerical value of skin friction coefficient $-f''(0)$ against M, Ω, Nc, Nr, Re, α, and β.

M	Ω	Nc	Nr	Re	α	β	$-f''(0)$
0.2							0.6678
0.8	0.5	0.5	0.5	0.5	1.0	−1.0	0.6795
1.4							0.6829
	0.1						0.6801
	0.2						0.6772
	0.3						0.6735
		0.1					0.6647
		0.6					0.6643
		1.2					0.6641
			1.0				0.6685
			2.0				0.6755
			3.0				0.6877
				0.4			0.6691
				0.8			0.6485
				1.2			0.6274
					0.1		0.6643
					0.2		0.4950
					0.3		0.3923
						−2.0	0.5224
						−3.0	0.4416
						−4.0	0.3874

Table 3. Numerical values of local Nusselt number $-\theta'(0)$ against Nb, Nt, Bi, Pr, Λ, Re and Ω.

Nb	Nt	Bi	Pr	Λ	Re	Ω	$-\theta'(0)$
0.4							0.2826
0.8							0.2821
1.0							0.2812
	0.4						0.2780
	0.7						0.2676
	1.0						0.2573
		3.0					0.2958
		4.0					0.3035
		5.0					0.3084
			0.7				0.2386
			0.9				0.2677
			1.1				0.2947
				0.2			0.2931
				0.5			0.3182
				0.8			0.3361
					0.4		0.2858
					0.8		0.2702
					1.2		0.2585
						0.1	0.3001
						0.2	0.2952
						0.3	0.2904

Table 4. Variation in local Sherwood number $-\phi'(0)$ against Nb, Nt, Le, Bi, Λ, Ra, Ω and Pr.

Nb	Nt	Le	Λ	Re	Ω	Pr	$-\phi'(0)$
0.4							0.2120
0.8							0.1263
1.0							0.0850
	0.4						0.5560
	0.7						0.9367
	1.0						1.2865
		3.0					0.4215
		4.0					0.4209
		5.0					0.4204
			0.2				0.4397
			0.5				0.4773
			0.8				0.5041
				0.4			0.4287
				0.8			0.4052
				1.2			0.3877
					0.1		0.4502
					0.2		0.4427
					0.3		0.4355
						0.7	0.3578
						0.9	0.4016
						1.1	0.4420

Table 5. Numerical values of density motile microorganisms $-\chi'(0)$ against *Pe*, *M*, *Lb*, Λ, *Nr*, *Nc*, Re and Ω.

Pe	*Lb*	*M*	Λ	Nr	Nc	Re	Ω	$-\chi^{'}(0)$
0.3								0.9872
0.5	2.0	0.1	0.1	0.5	0.5	0.5	0.5	1.1321
0.7								1.2802
	3.0							1.0953
0.1	4.0							1.3104
	5.0							1.5035
		0.2						0.8233
		0.8						0.7173
		1.4						0.6446
			0.2					0.8749
			0.5					0.9416
			0.8					0.9922
				1.0				0.8413
				2.0				0.8310
				3.0				0.8173
					0.1			0.8544
					0.6			0.8434
					1.2			0.8294
						0.4		0.8610
						0.8		0.8044
						1.2		0.7606
							0.1	0.9105
							0.2	0.8936
							0.3	0.8771

6. Conclusions

In this investigation, the bioconvection flow of third-grade nanofluid over a moving stretched surface was inspected numerically. Additionally, the study was impacted by some external features, like magnetic force, viscous dissipation and activation energy. The study reports the following interesting observations:

- A lower velocity profile is observed with interaction of buoyancy ratio constant and slip parameters.
- The change in material parameters depressed the nanoparticles' temperature effectively.
- The temperature profile gets maximum variation with thermophoresis parameter, Biot number and radiation constant.
- It further emphasizes that rate of mass transportation can be controlled by increasing Schmidt number and Brownian motion parameter.
- It is claimed that the presence of slip factors is more useful to improve the combined heat and mass transportation and motile microorganisms' density profiles.
- It is further examined that presence of material parameters reduces the motile microorganisms' density profiles.

Author Contributions: All authors contribute in all works steps and phases equally from beginning to publication. All authors have read and agreed to the published version of the manuscript.

Funding: This research received no external funding"

Conflicts of Interest: The authors declare no conflict of interest.

Nomenclature

(u,v) velocity components
ν is kinematic viscosity,
β_3 being third-grade fluid parameter,
g^* gravity,
ρ_m is the microorganisms' particles' density,
C represents the concentration,
α_e thermal diffusivity,
σ^* Stephan-Boltzmann,
$(\rho c)_p$ effective heat capacity of nanoparticles,
D_T thermodiffusion constant,
Boltzmann constant,
W_e is speed of cells
h_f represents the heat transfer coefficient
k_n, Knudsen number
ε molecular mean free path
K is material parameter,
Nr buoyancy ratio parameter,
Re is Reynolds number,
Pr Prandtl number,
Nb Brownian motion parameter,
Ec Eckert number,
σ^{**} is reaction constant
E activation energy parameter
Pe Peclet number
Bi thermal Biot number
β second-order slip constants
α_1 material parameter,
ρ_f is the fluid density,
β^* volume expansion coefficient
ρ_p is the nanoparticles density,
T is the temperature,
N microorganisms' density,
k^* mean absorption coefficients,
$(\rho c)_f$ is effective heat capacity of base fluid,
D_B reports the diffusion constant,
$K_1 r$ reaction rate, κ
E_a activation energy,
b_1 denotes the chemotaxis constant.
T_f convective fluid temperature
Λ momentum coefficient
M is Hartmann number
Λ mixed convection parameter,
Nc bioconvection Rayleigh number
Ω is third-grade fluid parameter
Rd radiation parameter
Nt thermophoresis parameter
Le Lewis number
δ temperature difference parameter
δ_1 specify microorganism concentration difference constant
Lb determine the bioconvection Lewis number
α first-order slip and

References

1. Choi, S.U.S. Enhancing thermal conductivity of fluids with nanoparticles. *ASME Pub. Fed.* **1995**, *231*, 99–106.
2. Buongiorno, J. Convective transport in nanofluids. *J. Heat Transf.* **2006**, *128*, 240–250. [CrossRef]
3. Sandeep, N.; Sulochana, C. Momentum and heat transfer behaviour of Jeffrey, Maxwell and Oldroyd-B nanofluids past a stretching surface with non-uniform heat source/sink. *Ain Shams Eng. J.* **2018**, *9*, 517–524. [CrossRef]
4. Pal, D.; Mandal, G. Thermal radiation and MHD effects on boundary layer flow of micropolar nanofluid past a stretching sheet with non-uniform heat source/sink. *Int. J. Mech. Sci.* **2016**, *126*, 308–318. [CrossRef]
5. Khan, M.; Irfan, M.; Khan, W.A. Impact of heat source/sink on radiative heat transfer to Maxwell nanofluid subject to revised mass flux condition. *Results Phys.* **2018**, *9*, 851–857. [CrossRef]
6. Hayat, T.; Rashid, M.; Khan, M.I.; Alsaedi, A. Melting heat transfer and induced magnetic field effects on flow of water based nanofluid over a rotating disk with variable thickness. *Results Phys.* **2018**, *9*, 1618–1630. [CrossRef]
7. Tlili, I.; Khan, W.A.; Khan, I. Multiple slips effects on MHD SA-Al2O3 and SA-Cu non-Newtonian nanofluids flow over a stretching cylinder in porous medium with radiation and chemical reaction. *Results Phys.* **2018**, *8*, 213–222. [CrossRef]
8. Khan, S.U.; Shehzad, S.A. Brownian movement and thermophoretic aspects in third grade nanofluid over oscillatory moving sheet. *Phys. Scr.* **2019**, *94*, 095202. [CrossRef]
9. Waqas, H.; Imran, M.; Khan, S.U.; Shehzad, S.A.; Meraj, M.A. Slip flow of Maxwell viscoelasticity-based micropolar nano particles with porous medium: A numerical study. *Appl. Math. Mech.* **2019**, *40*, 1255–1268. [CrossRef]
10. Hsiao, K. Micropolar nanofluid flow with MHD and viscous dissipation effects towards a stretching sheet with multimedia feature. *Int. J. Heat Mass Transf.* **2017**, *112*, 983–990. [CrossRef]

11. Sheikholeslami, M.; Bhatti, M.M. Forced convection of nanofluid in presence of constant magnetic field considering shape effects of nanoparticles. *Int. J. Heat Mass Transf.* **2017**, *111*, 1039–1049. [CrossRef]
12. Turkyilmazoglu, M. Fully developed slip flow in a concentric annuli via single and dual phase nanofluids models. *Comput. Methods Programs Biomed.* **2019**, *179*, 104997. [CrossRef] [PubMed]
13. Kuznetsov, A.V. The onset of nanofluid bioconvection in a suspension containing both nanoparticles and gyrotactic microorganisms. *Int. Commun. Heat Mass Transf.* **2010**, *37*, 1421–1425. [CrossRef]
14. Kuznetsov, A.V. Nanofluid bioconvection in water-based suspensions containing nanoparticles and oxytactic microorganisms: Oscillatory instability. *Nanoscale Res. Lett.* **2011**, *6*, 100. [CrossRef] [PubMed]
15. Uddin, M.J.; Alginahi, Y.; Bég, O.A.; Kabir, M.N. Numerical solutions for gyrotactic bioconvection in nanofluid-saturated porous media with Stefan blowing and multiple slip effects. *Comput. Math. Appl.* **2016**, *72*, 2562–2581. [CrossRef]
16. Xun, S.; Zhao, J.; Zheng, L.; Zhang, X. Bioconvection in rotating system immersed in nanofluid with temperature dependent viscosity and thermal conductivity. *Int. J. Heat Mass Transf.* **2017**, *111*, 1001–1006. [CrossRef]
17. Raju, C.S.K.; Hoque, M.M.; Sivasankar, T. Radiative flow of Casson fluid over a moving wedge filled with gyrotactic microorganisms. *Adv. Powder Technol.* **2017**, *28*, 575–583. [CrossRef]
18. Alsaedi, A.; Khan, M.I.; Farooq, M.; Gull, N.; Hayat, T. Magnetohydrodynamic (MHD) stratified bioconvective flow of nanofluid due to gyrotactic microorganisms. *Adv. Powder Technol.* **2017**, *28*, 288–298. [CrossRef]
19. Khan, W.A.; Rashad, A.M.; Abdou, M.M.M.; Tlili, I. Natural bioconvection flow of a nanofluid containing gyrotactic microorganisms about a truncated cone. *Eur. J. Mech. B Fluids* **2019**, *75*, 133–142. [CrossRef]
20. Alwatban, A.M.; Khan, S.U.; Waqas, H.; Tlili, I. Interaction of Wu's slip features in bioconvection of Eyring Powell nanoparticles with activation energy. *Processes* **2019**, *7*, 859. [CrossRef]
21. Tlili, I.; Waqas, H.; Almaneea, A.; Khan, S.U.; Imran, M. Activation energy and second order slip in bioconvection of Oldroyd-B nanofluid over a stretching cylinder: A proposed mathematical model. *Processes* **2019**, *7*, 914. [CrossRef]
22. Xu, H.; Pop, I. Fully developed mixed convection flow in a horizontal channel filled by a nanofluid containing both nanoparticles and gyrotactic microorganisms. *Eur. J. Mech. B Fluids* **2014**, *46*, 37–45. [CrossRef]
23. Pop, M.A.S.I. Thermo-Bioconvection in a Square Porous Cavity Filled by Oxytactic Microorganisms. *Transp. Porous Med.* **2014**, *103*, 191. [CrossRef]
24. Dunn, J.E.; Rajagopal, K.R. Fluids of differential type: Critical review and thermodynamic analysis. *Int. Jr. Eng. Sci.* **1995**, *33*, 689–729. [CrossRef]
25. Ali, N.; Khan, S.U.; Abbas, Z. Unsteady Flow of Third Grade Fluid over an Oscillatory Stretching Sheet with Thermal Radiation and Heat Source/Sink. *Nonlinear Eng.* **2015**, *4*, 223–236. [CrossRef]
26. Ali, N.; Ullah, M.; Sajid, M.; Khan, S.U. Application of Legendre wavelets method to parallel plate flow of a third grade fluid and forced convection in a porous duct. *Eur. Phys. J. Plus* **2017**, *132*, 133. [CrossRef]
27. Abbas, Z.; Javed, T.; Ali, N.; Sajid, M. Diffusion of Chemically Reactive Species in Stagnation-Point Flow of a Third Grade Fluid: A Hybrid Numerical Method. *J. Appl. Fluid Mech.* **2016**, *9*, 195–203. [CrossRef]
28. Wu, L. A slip model for rarefied gas flows at arbitrary Knudsen number. *Appl. Phys. Lett.* **2008**, *93*, 253103. [CrossRef]
29. Waqas, H.; Khan, S.U.; Hassan, M.; Bhatti, M.M.; Imran, M. Analysis for bioconvection flow of modified second grade fluid containing gyrotactic microorganisms and nanoparticles. *J. Mol. Liq.* **2019**, *291*, 111231. [CrossRef]
30. Khan, S.U.; Waqas, H.; Shehzad, S.A.; Imran, M. Theoretical analysis for tangent hyperbolic nanoparticles with combined electrical MHD, activation energy and Wu's slip features: A mathematical model. *Phys. Scr.* **2019**, *94*, 125211. [CrossRef]
31. Ibrahim, W. Magnetohydrodynamics (MHD) flow of a tangent hyperbolic fluid with nanoparticles past a stretching sheet with second order slip and convective boundary condition. *Results Phys.* **2017**, *7*, 3723–3731. [CrossRef]
32. Turkyilmazoglu, M. The analytical solution of mixed convection heat transfer and fluid flow of a MHD viscoelastic fluid over a permeable stretching surface. *Int. J. Mech. Sci.* **2013**, *77*, 263–268. [CrossRef]